An improved WOA of PI control for three phase PWM rectifier

Shwetha G, Guruswamy K P
Department of Electrical and Electronics Engineering, UVCE, Bangalore University, Bengaluru, India

Article Info

ABSTRACT

In the empire of electric vehicle (EV) propulsion systems, efficient energy conversion is paramount for extending driving range and enhancing overall performance. Rectifiers play a crucial role in converting AC from the grid into DC for battery charging and motor operation. However, the performance of rectifiers is heavily influenced by the control algorithms employed. This work presents an optimized proportional-integral (PI) controller design for rectifiers in EV applications. The proposed controller aims to achieve high efficiency, fast response, and robustness to variations in load and input voltage. The optimization process incorporated in this work utilized whale optimization topology for tuning the PI controller parameters. The objective is to minimize cost function that represents deviation of rectifier output from desired characteristics under various operating conditions. The outcomes of simulation demonstrate that suggested controller works to provide greater accuracy than traditional control techniques. Moreover, experimental validation verifies the proposed controller's reliability and efficiency in practical EV applications. The optimized PI controller contributes to maximizing energy efficiency, extending battery life, and enhancing the overall reliability of electric vehicle propulsion systems.

Corresponding Author:

Shwetha G
Department of Electrical and Electronics, UVCE, Bangalore University
Bengaluru, India
Email: m.g.shwetha99@gmail.com

1. INTRODUCTION

In the field of power electronics, rectification plays a crucial element role that has great importance. A wide range of rectifiers are created as technology develops. Different classifications are revealed by depending on their basic circuit structures, which are as follows:
− Single phase rectification,
− Three-phase rectification.

Among these, 1ϕ rectifiers offer simplicity and cost-effectiveness, but they exhibit relatively large output ripple [1]-[5]. Conversely, 1ϕ full wave rectifiers exhibit small output ripple and high efficiency. On the other hand, 3ϕ rectifiers deliver stable and efficient output voltage. Different types of rectifiers are used in different situations, but compared to single phase converter three-phase full-wave rectification circuits which incorporate pulse width modulation (PWM) techniques commonly used in many applications related to electric vehicle charging. because they have a unity power factor correction, a low distortion of harmonic content, and a sinusoidal input current, among other benefits [6]-[10].

However, 3ϕ PWM rectifier's open loop control requires changing the 3ϕ power supply using PWM modulation in order to control the rectifier's output voltage. Open loop control is resulting in inaccurate.

In the rotating coordinate (dq) system for PWM rectifier scheme of control, measuring direct current techniques and double schematic closed loop topologies are frequently used to overcome this constraint [11]-[16].

When the output voltage fluctuates under technique control, the controller quickly finds out's any changes throughout feedback loop and makes modifications. The DC side rapidly recover to the desired value due to this extent [17]-[20]. PWM rectifiers can be rendered more precise and stable by using this technique, which makes it appropriate for applications requiring a high accurate and constant output voltage.

The control strategy comprises an inside current loop to control output and phase of grid-side current, and an outside voltage loop to control rectifier's output voltage [21]. After undergoing reverse transformation, the command is converted into a trigger signal.

The technology demonstrates outstanding future of PWM rectifiers in different fields of renewable energy with its high efficiency in pointing out the maximum power point and maintaining minimal harmonic distortion (THD) [22]. Hence to achieve the stability and system reliableness, researchers conducted theoretical investigations and established a corresponding diagnostic scheme in dealing with the problem of 1ϕ open line faults in a 3ϕ PWM rectifier [23].

A feedback control method based on capacitive energy storage was developed; it comprised of an outside loop (capacitive energy storage) and an inner loop (current). Through employing this approach, the system's dynamic properties become gradually improved and delayed output voltage regulation during load changes are prevented [24]. In a similar stream, an inner loop consisting of current and an outer loop with voltage doubled situation is developed to maximize the rectifier's efficiency [25].

While, integral windup is a major limitation of a PI controller. This part develops when the integral term continues to produce errors even when the system is saturated or incapable of reacting due to constraints or physical restrictions. When the control signal saturates, the integral term keeps integrating the error, leading to overshoot or oscillations when the system becomes active again. This phenomenon can degrade control performance, especially in systems with large set point changes or disturbances. Thus, to overcome this problem, an optimization of PI controller parameters have be adopted. Keeping this in view, this work formulated a novel optimized topology called whale optimization to optimize the PI controller adopted in the Rectifier circuit.

2. ANALYSIS AND MODELING OF THREE-PHASE TOPOLGY

The primary circuit of the three-phase voltage source PWM rectifier circuit is shown in Figure 1, here Ia, Ib, and Ic determine the input source current of grid-side and Ua, Ub, and Uc indicates power-supply voltage of each phase. The filter inductance is represented by L_s, load resistance is denoted by R_L, DC-side output voltage is indicated by Udc, output current is depicted by Idc, the filter-inductance equivalent resistance is suggested as R_s, and IGBT with freewheeling diodes is stated as switch 1-6.
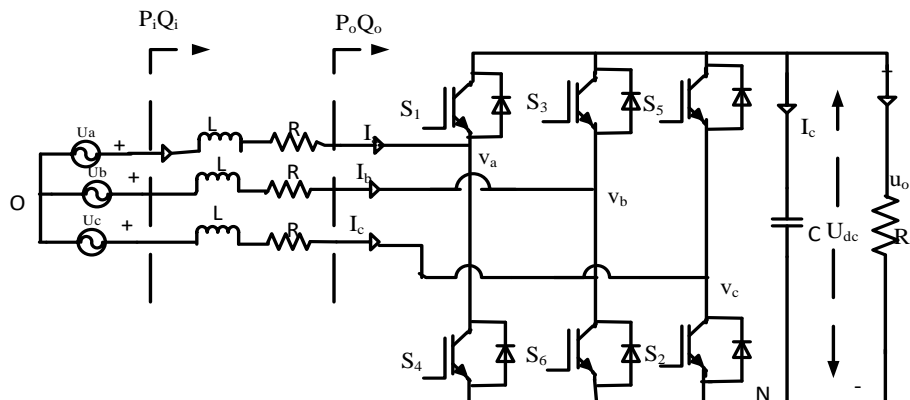

Figure 1. Topology of the main circuit of the three-phase bridge rectifier

To understand working principle and system control, the three-phase PWM rectifier's input side and output mathematical model should be developed. In the beginning, the circuit parameters are measured using the KVL and KCL equations to obtain:

$$-E_a + R_s i_{sa} + L_s \frac{di_{sa}}{dt} + u_{ao} = 0$$
$$-E_b + R_s i_{sb} + L_s \frac{di_{sb}}{dt} + u_{bo} = 0$$
$$-E_c + R_s i_{sc} + L_s \frac{di_{sc}}{dt} + u_{co} = 0$$
$$C \frac{du_{dc}}{dt} + \frac{U_{dc}}{R} = i_{dc} \tag{1}$$

The outcomes that follow properties of a power supply from three-phase can be obtained. if the switching value Sj (j=a,b,c) is applied in place of u jo (j=a,b,c) where formula (Sj=1 preferred as upper bridge arm conduction in j phase; Sj = 0 implies lower bridge part operation):

$$E_a + E_b + E_c = 0.$$
$$L_s \frac{di_{sa}}{dt} = E_a - R_s i_{sa} - s_a - \frac{1}{3}[S_a + S_b + S_c]U_{dc}$$
$$L_s \frac{di_{sb}}{dt} = E_b - R_s i_{sb} - s_b - \frac{1}{3}[S_a + S_b + S_c]U_{dc}$$
$$L_s \frac{di_{sc}}{dt} = E_c - R_s i_{sc} - s_c - \frac{1}{3}[S_a + S_b + S_c]U_{dc}$$
$$C \frac{du_{dc}}{dt} = i_a s_a + i_b s_b + i_c s_c - \frac{u_{dc}}{R}$$

The mathematical model expressions from 3ϕ constant coordinate arrangement of PWM rectifier and with four formulas in the equation, designing a control system becomes unnecessarily complicated. Mathematical modification is therefore still required. The transition between the dq rotating reference frame and abc three-phase stationary-coordinate system are considered as solution. A PWM rectifier's control becomes substantially more complex because the variables on the alternating side are time-changing. To solve this issue, a coordinated transformation into a synchronous rotation correlate procedure (dq) is suggested as a method to simplify control requirements.
- Controller design

The PI controller is used for control, with ud, uq as the output and id, iq for input response. It can be derived in such a way that incorporates feedforward decoupling into account:

$$u_d = (i_d - i_d^*)(K_p + \frac{k_i}{s}) + \omega L_s i_q + e_d$$
$$u_q = (i_q - i_q^*)(K_p + \frac{k_i}{s}) + \omega L_s i_q + e_q \tag{3}$$

where Kp and Ki represent the coefficient of proportion and integration for the PI controller respectively.

It is possible to create a controller with an internal-current loop by using (3). the system-block diagram is shown in detail in Figure 2. The current configuration, as shown in the diagram, demonstrates a closed loop using the system's current id and iq. the power technique fails to respond with the DC voltage of load side. instead, current-closed loop is present in the primary control loop, which is also referred as voltage-closed loop. hence referred as the outer loop of voltage, and inside control process, which controls current, is called the inner-current loop.
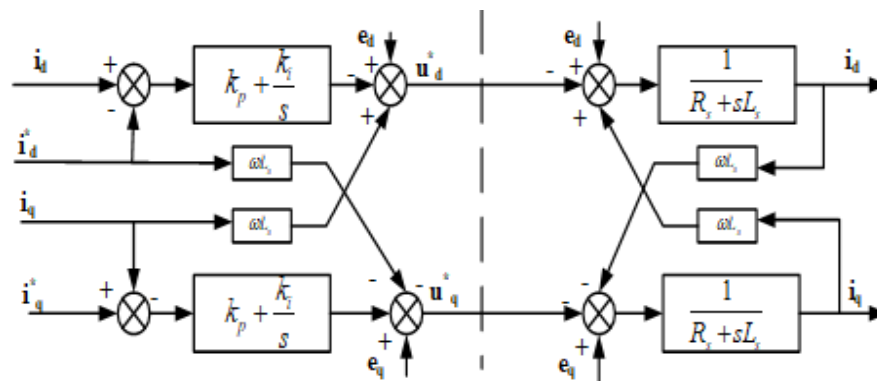

Figure 2. Design of the controller

The voltage-closed loop control process can be described by following (4):

$$udc *= Kp(udc * -udc) + Ki \int (udc * -udc)dt \tag{4}$$

Where:
udc∗: reference voltage
udc: actual voltage
Kp: proportional gain
Ki: integral part

The above utilized controller receives error signal (udc∗−udc) in this control scheme and determines the control signal id to modify DC side voltage. While the integral term helps in removing any steady-state error, the proportional term modifies output in accordance with the present error. The current in system's d-axis is then controlled by PI controller's output, id, allows modifications to the voltage on output load side. The control segment can interact with the DC side voltage fluctuations and regulate them in accordance with reference voltage Udc these are advantages of voltage-closed loop control mechanism. Likewise, the definition of a current controller is as:

$$i_d = \left(K_p' + \frac{k_i'}{s} \right) (u_{dc}^* - u_{dc}) \tag{5}$$

The 3ϕ PWM rectifier's entire block diagram is shown in Figure 3. The rectifier's DC-side voltage is stabilized and kept constant by the outside voltage loop. Reactive component (iq) is set for zero in order to preserve unity PF content. Subsequently, feedback values corresponding to the current element on dq-axis are compared with active current (id) and reactive current (iq) separately. These are the comparisons that follow the PI regulator. The rectifier's switching states are then controlled by a space-vector modulator while the output has undergone vector translation. This procedure causes the rectifier's AC-side current waveform to become sinusoidal, which makes it easier to manage and reach unity PF.
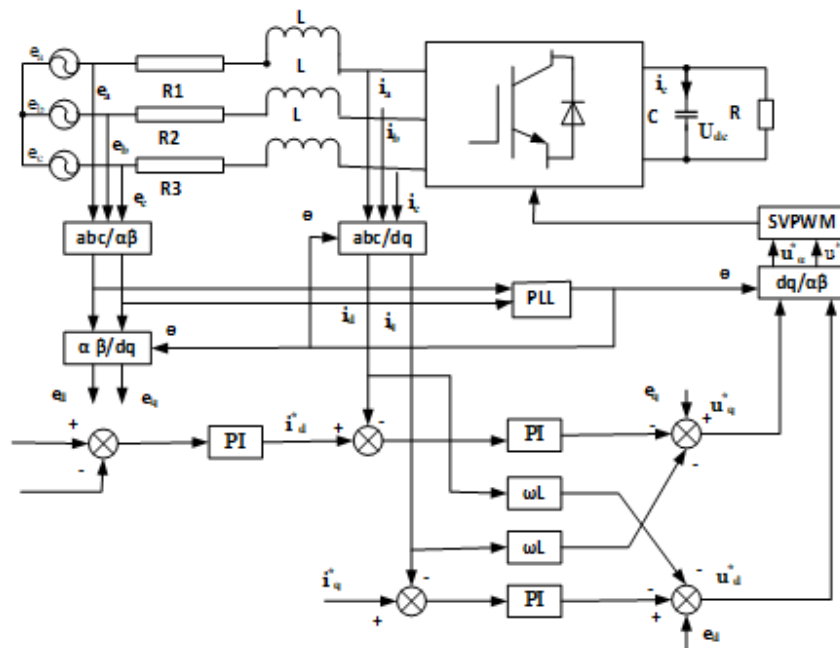

Figure 3. Control scheme-structural diagram of proposed rectifier

Many advantages come with this control method, such as its great steady-state performance, quick dynamic reaction, and in-built protection for current-limit. Additionally, it achieves unity PF and successfully removes current-steady-state faults, making it more appropriate for a variety of applications. In addition, this study has devised a novel stepped voltage setting approach to improve control efficacy. Therefore, optimization topology has been examined in order to further increase the PI controller's efficiency.

3.   WHALE OPTIMIZATION ALGORITHM FOR PI TUNING

The concept of WOA originates from the Bubble-net attacking strategy, where whales corral fish by creating spiral-shaped air pockets around them up to 12 meters below the water's surface, then ascending to trap and capture their targeted prey shortly after. In terms of whale observations, the methodological approach is reflected in this algorithm through the complex search for food, which stay scientifically clarified by resurrecting past patterns rather than arbitrarily selecting alternative courses of action which is shown in Figure 4. Despite this impactful behavior, WOA distinguishes itself from other improvement strategies because it only necessitates two boundary adjustments. These boundaries facilitate smooth transitions between exploitation and exploration frameworks.
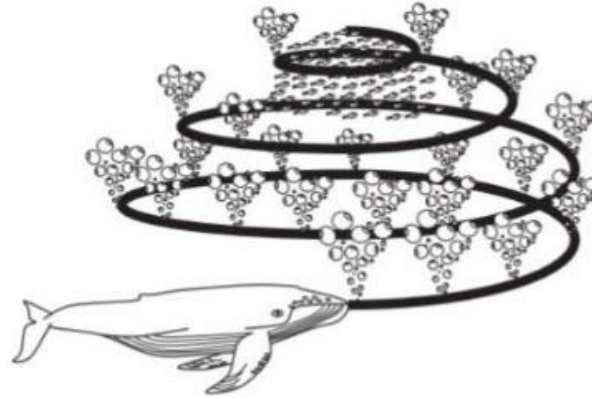

Figure 4. Finding attack prey technique

The segment ahead will demonstrate model for encircling prey, searching for prey, and employing the air-filled pocket net of scavenging action. The behavior of humpback whales surrounding prey and updating their situation to optimize their chase can be quantified as follows: As the number of cycles increases from the initial stages to the most extreme numbers, humpback whales engage in a coordinated effort to encircle the prey. During this process, they dynamically adjust their positions and tactics to maximize their efficiency in chasing and capturing the prey.
On the off chance that ($p<0.5$ and mod (U) <1)
At that point, the situation of competitor position X (t+1) is refreshed by the accompanying conditions:

$$D = \text{mod} \{(C.X) - X(t)\}$$
$$X(t+1) = [X(t) - \{U.D\}] \tag{6}$$

Where p =0.1 (consistent).
X (t+1) is the best situation in the current circumstance. U and C are determined by accompanying conditions:
U= mod {2.a.r-a}
C=2.r
Where a is directly diminishes from 2 to 0 and r is the haphazardly chosen vector. Prey Searching equations are given as follows:

$$D = \text{mod} \{(C.Xrandom) - X(t)\}$$
$$X(t+1) = [Xrandom(t) - \{U.D\}] \tag{7}$$

During the inquiry phase of whale advancement computation, the surrounding and winding refreshing of prey were completed. set the zero values to population number, design variables, and maximum numeral of iterations. For each design variable, find the fitness function for each search agent. The other one should next try to modify their positions to match best fit, or optimal solution, as seen in Figure 5. Adjust each search agent's position by doing the following: When P is less than 0.5, and p is a random number between 0 and 1.
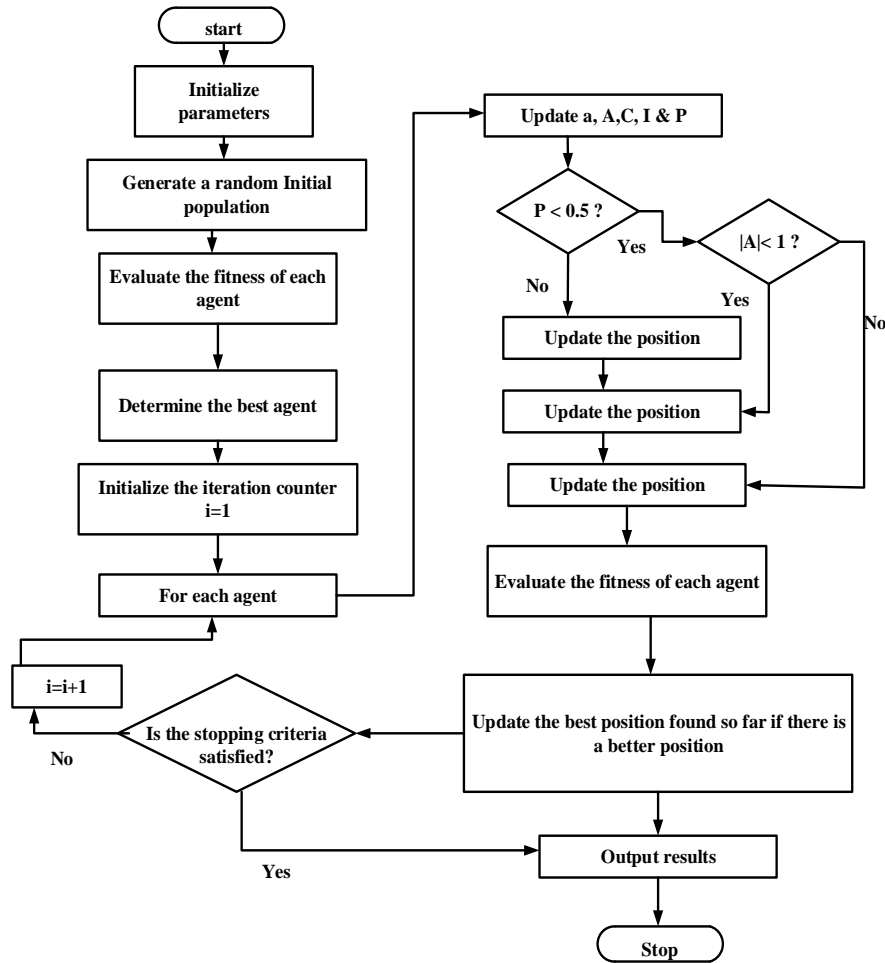
Figure 5. Whale optimization implementation flow diagram

4.   RESULTS AND DISCUSSION

A MATLAB/Simulink simulation was performed to confirm that the established model was appropriate. Integrating a voltage outer loop and a current inner loop is become most common approach for control technique. The PI parameters can be obtained by using the current loop to derive its open loop transfer function. The obtained trans-function can be utilized for voltage outer loop and PI value calculations related to voltage loop. These variables are first computed and are used as a basis for additional fine-tuning to produce ideal results. The relevant circuit measurements are provided in Table 1.

Table 1. Circuit parameters

Circuit Parameter	Value
Voltage (V)	380 V
R_s	$40 m\Omega$
L_s	$1\ mH$
Capacitance	$6800\ uF$
Voltage K_p	0.05
Voltage K_i	79
Current K_p	0.2
Current K_i	45

The effectiveness of the PWM rectifier employing the newly suggested controller is evaluated across four distinct operating scenarios, considering metrics like rise time (t_r), settling time (t_s), and PF. The different operating conditions are given in below.

4.1. Under condition 1

The voltage across output side i.e load side observed during simulation is shown in Figure 6. It shows that when output voltage which is derived from control mechanism of dual closed loop scheme is set at 800 V, DC side voltage can reach the steady state value in 0.058 seconds and become stable. The output voltage has an effect when the R_L value of load suddenly changes at 0.25 seconds, but it quickly returns to the desired value in 0.05 seconds.

Figure 7 depicts the observation of source voltage and current waveforms on input side. At 0.25 seconds in simulation, the load resistance suddenly halved, effects as development in current magnitude. Despite this change, the Is on the source side closely resembled a sine wave with minimal distortion. Furthermore, the Vs and Is consistently followed in phase, indicating maintenance of unity PF. As a result, there was only less pollution on the grid side, validating the uses of PWM based rectifier discussed earlier in this article.
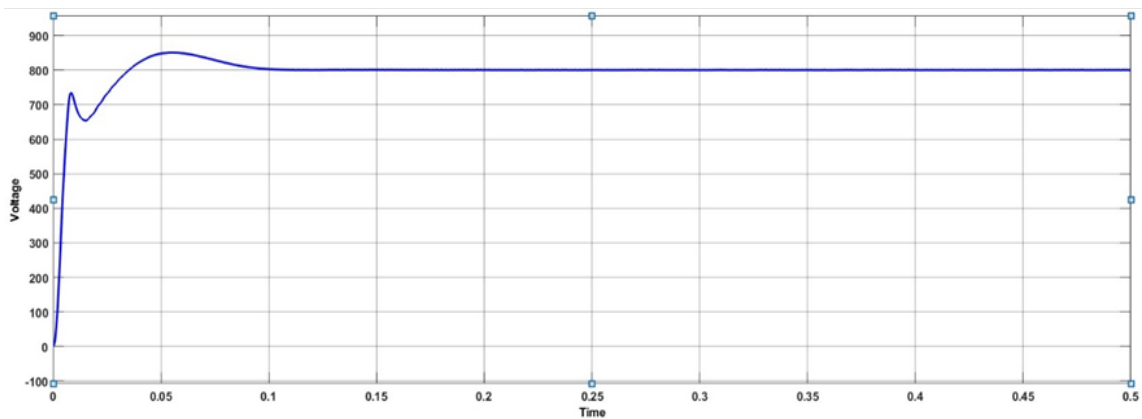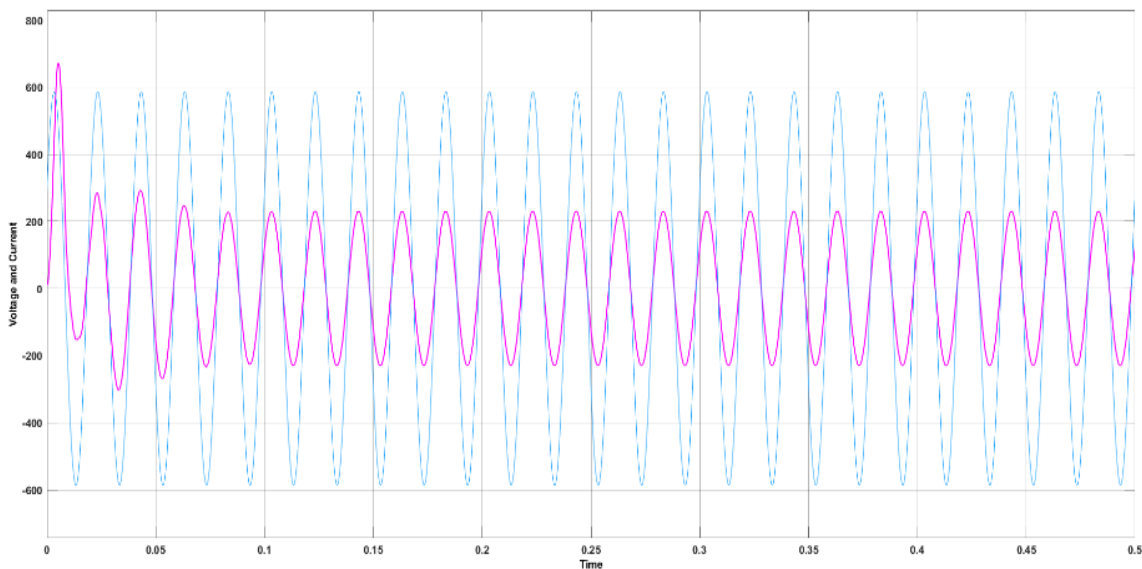

Figure 6. DC-output-voltage waveform

Figure 7. Voltage and current waveform on grid side

4.2. Condition-2

Figure 8 illustrates the behavior of rectifier structure under step change in input side. When rectifier at steady condition, the unbalanced state in AC supply happens between t = 0.4 and up to 0.6 seconds. The result shows that the DC-link voltage varies around its reference value in both controller scenarios.
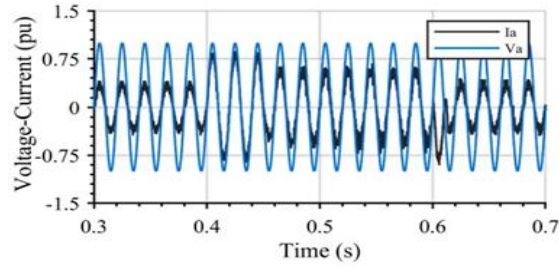
Figure 8. Simulation results of step change operation

4.3. Condition-3

Figure 9 depicts the response of the system unbalanced AC supply. it cleared for the image that when there is a change sudden changes from input side there is two changes at 0.39 and also large changes from 0,55 to 0.65. Hence conclude that supply changes leads to different variations.
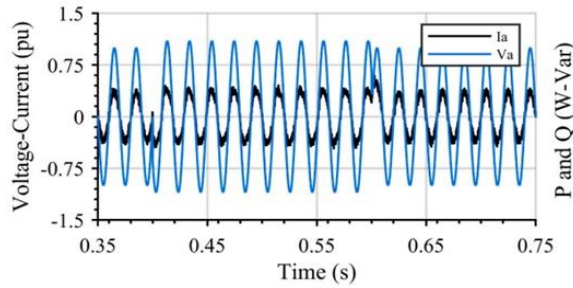

Figure 9. Simulation results of unbalanced AC supply operation

4.4. Condition-4

This case study investigates the effects of load changes on the DC side of a rectifier. Specifically, it examines the impact of reducing the load by 50%.the Figure 10 shows effects. From all the cases, it is evident that proposed controller maintains a constant DC link voltage around its pre-defined reference value. This, the performance of the controller under various condition is depicted in Table 2.
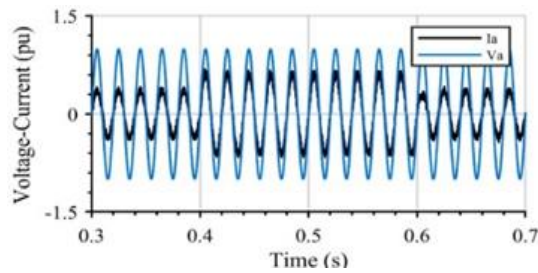

Figure 10. Simulation results of load change operation

Table 2. Performance measures

Criteria	t_r	ts	PF
Condition 1	0.0126	0.06	0.99
Condition 2	0.0132	0.072	0.98
Condition 3	0.0040	0.0138	0.98
Condition 4	0.020	0.014	0.98

4.5. Implementation results

The validation of the simulation study occurs through experimentation on a 3-phase active rectifier laboratory setup. In the initial investigation aimed at assessing the proposed method's steady-state performance, experimental outcomes under various DC voltage set points are depicted in Figure 11.

Figure 12 Throughout this examination, two set points, namely 715 and 800 V, are tested. The results indicate a maximum instantaneous error is very less and consequently deduced that the proposed method yields a steady-state error close to zero across a broad range of DC voltage variations.

Moreover, Figure 13 displays a zoomed-in voltage ripple during full load operation. As a result, in the worst situation (full load operation), the voltage ripple is less than 3%, demonstrating the enhanced effectiveness of the suggested control strategy.
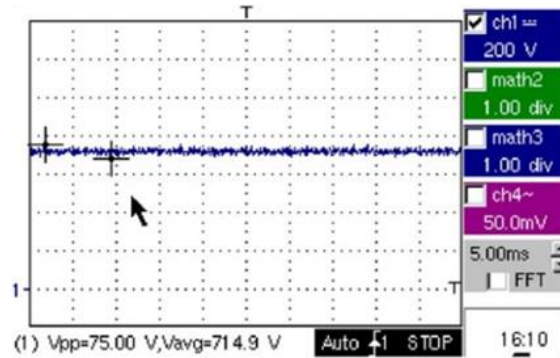

Figure 11. Experimental results under steady state condition with DC voltage set point at 715 v
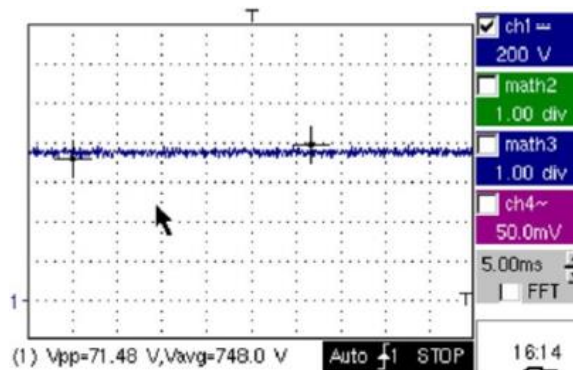

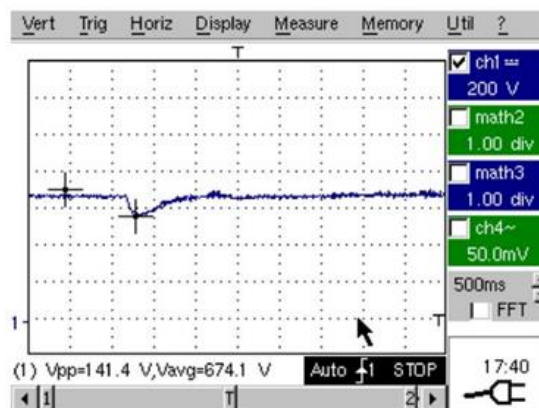
Figure 12. Experimental results at 800 v

Figure 13. The dynamic response of proposed control algorithm (under load change)

Consequently, it can be inferred that the suggested approach yields a steady state error close to zero. Additionally, which also depicts the THD during full load operation. Consequently, the voltage ripple under the most demanding conditions (full load operation) is confirmed to be less than 3%, validating the exceptional performance of the proposed control method.

5. CONCLUSION

There are many uses for the three-phase voltage source PWM rectifier in power electronics systems, and researchers are always working to improve its control schemes. The mathematical model for input side and output of a proposed PWM rectifier is derived in this study. The control technique performs exceptionally well dynamically and quickly adapts to variations in load by resetting to a predetermined value. Moreover, it efficiently creates a sinusoidal waveform out of the network-side current, reducing harmonic pollution and preserving unity PF functioning. When compared to conventional procedures, this technology offers improved operability and flexibility. The main goal in this project is to increase dynamically and static state performance of above suggested PWM rectifiers for real-world applications by extending their effective voltage-control range.

REFERENCES

[1] Z. Li, Y. Li, P. Wang, H. Zhu, C. Liu, and W. Xu, "Control of three-phase boost-type PWM rectifier in stationary frame under unbalanced input voltage," *IEEE Transactions on Power Electronics*, vol. 25, no. 10, pp. 2521–2530, Oct. 2010, doi: 10.1109/TPEL.2010.2049030.

[2] C. Li, J. Hu, and M. Zhao, "Grid-voltage sensorless predictive current control of three-phase PWM rectifier with fast dynamic response and high accuracy," *CPSS Transactions on Power Electronics and Applications*, vol. 8, no. 3, pp. 269–277, Sep. 2023, doi: 10.24295/CPSSTPEA.2023.00037.

[3] A. Rahoui, A. Bechouche, H. Seddiki, and D. O. Abdeslam, "Grid Voltages Estimation for Three-Phase PWM rectifiers control without AC voltage sensors," *IEEE Transactions on Power Electronics*, vol. 33, no. 1, pp. 859–875, Jan. 2018, doi: 10.1109/TPEL.2017.2669146.

[4] A. M. Bozorgi, H. Gholami-Khesht, M. Farasat, S. Mehraeen, and M. Monfared, "Model predictive direct power control of three-phase grid-connected converters with fuzzy-based duty cycle modulation," *IEEE Transactions on Industry Applications*, vol. 54, no. 5, pp. 4875–4885, Sep. 2018, doi: 10.1109/TIA.2018.2839660.

[5] T. Na, X. Yuan, J. Tang, and Q. Zhang, "A review of on-board integrated charger for electric vehicles and a new solution," in *PEDG 2019 - 2019 IEEE 10th International Symposium on Power Electronics for Distributed Generation Systems*, IEEE, Jun. 2019, pp. 693–699. doi: 10.1109/PEDG.2019.8807565.

[6] J. W. Kolar, T. Friedli, J. Rodriguez, and P. W. Wheeler, "Review of three-phase PWM AC-AC converter topologies," *IEEE Transactions on Industrial Electronics*, vol. 58, no. 11, pp. 4988–5006, Nov. 2011, doi: 10.1109/TIE.2011.2159353.

[7] W. S. Im, J. M. Kim, D. C. Lee, and K. B. Lee, "Diagnosis and fault-tolerant control of three-phase AC-DC PWM converter systems," *IEEE Transactions on Industry Applications*, vol. 49, no. 4, pp. 1539–1547, Jul. 2013, doi: 10.1109/TIA.2013.2255111.

[8] Y. Zhang, Z. Wang, J. Jiao, and J. Liu, "Grid-voltage sensorless model predictive control of three-phase PWM rectifier under unbalanced and distorted grid voltages," *IEEE Transactions on Power Electronics*, vol. 35, no. 8, pp. 8663–8672, Aug. 2020, doi: 10.1109/TPEL.2019.2963206.

[9] L. Tarisciotti, P. Zanchetta, A. Watson, S. Bifaretti, J. C. Clare, and P. W. Wheeler, "Active DC voltage balancing PWM technique for high-power cascaded multilevel converters," *IEEE Transactions on Industrial Electronics*, vol. 61, no. 11, pp. 6157–6167, Nov. 2014, doi: 10.1109/TIE.2014.2308139.

[10] W. Jiang, Y. Wang, J. P. Wang, L. Wang, and H. Huang, "Maximizing instantaneous active power capability for PWM rectifier under unbalanced grid voltage dips considering the limitation of phase current," *IEEE Transactions on Industrial Electronics*, vol. 63, no. 10, pp. 5998–6009, Oct. 2016, doi: 10.1109/TIE.2016.2577544.

[11] H. Zhang, X. Zhu, J. Shi, L. Tan, C. Zhang, and K. Hu, "Study on PWM rectifier without grid voltage sensor based on virtual flux delay compensation algorithm," *IEEE Transactions on Power Electronics*, vol. 34, no. 1, pp. 849–862, Jan. 2018, doi: 10.1109/TPEL.2018.2815019.

[12] A. Kouchaki and M. Nymand, "Analytical design of passive LCL filter for three-phase two-level power factor correction rectifiers," *IEEE Transactions on Power Electronics*, vol. 33, no. 4, pp. 3012–3022, Apr. 2018, doi: 10.1109/TPEL.2017.2705288.

[13] J. Xu, X. Li, H. Liu, and X. Meng, "Fractional-order modeling and analysis of a three-phase voltage source PWM rectifier," *IEEE Access*, vol. 8, pp. 13507–13515, 2020, doi: 10.1109/ACCESS.2020.2965317.

[14] X. Guo, H. P. Ren, and D. Liu, "An optimized PI controller design for three phase PFC converters based on multi-objective chaotic particle swarm optimization," *Journal of Power Electronics*, vol. 16, no. 2, pp. 610–620, Mar. 2016, doi: 10.6113/JPE.2016.16.2.610.

[15] M. Malinowski, M. Jasiński, and M. P. Kazmierkowski, "Simple direct power control of three-phase PWM rectifier using space-vector modulation (DPC-SVM)," *IEEE Transactions on Industrial Electronics*, vol. 51, no. 2, pp. 447–454, Apr. 2004, doi: 10.1109/TIE.2004.825278.

[16] X. Zhang *et al.*, "Single-phase three-level PWM rectifier predictive control with fixed switching frequency based on current convex optimization," *IEEE Transactions on Power Electronics*, vol. 36, no. 10, pp. 12090–12101, Oct. 2021, doi: 10.1109/TPEL.2021.3073532.

[17] S. Kakkar *et al.*, "Design and control of grid-connected PWM rectifiers by optimizing fractional order PI controller using water cycle algorithm," *IEEE Access*, vol. 9, pp. 125941–125954, 2021, doi: 10.1109/ACCESS.2021.3110431.

[18] T. Song, Y. Zhang, F. Gao, X. Zhu, J. Shan, and Z. Kong, "Power model free voltage ripple suppression method of three-phase PWM rectifier under unbalanced grid," *IEEE Transactions on Power Electronics*, vol. 37, no. 11, pp. 13799–13807, Nov. 2022, doi: 10.1109/TPEL.2022.3184403.

[19] P. Wang, Y. Bi, F. Gao, T. Song, and Y. Zhang, "An improved deadbeat control method for single-phase PWM rectifiers in charging system for EVs," *IEEE Transactions on Vehicular Technology*, vol. 68, no. 10, pp. 9672–9681, Oct. 2019, doi: 10.1109/TVT.2019.2937653.

[20] T. Wang *et al.*, "Single-Phase bridgeless three-level power factor correction topologies based on the embedded construction scheme," *IEEE Access*, vol. 11, pp. 109722–109733, 2023, doi: 10.1109/ACCESS.2023.3322648.

[21] S. Wang, L. Zhu, Y. Wang, J. Yang, Y. Zhou, and Z. Shu, "SVPWM voltage balancing boundary analysis and extension of single-phase cascaded multilevel rectifier," *IEEE Transactions on Power Electronics*, vol. 39, no. 7, pp. 8269–8280, Jul. 2024, doi: 10.1109/TPEL.2024.3381821.

[22] Z. Zeng, W. Zheng, R. Zhao, C. Zhu, and Q. Yuan, "Modeling, modulation, and control of the three-phase four-switch PWM rectifier under balanced voltage," *IEEE Transactions on Power Electronics*, vol. 31, no. 7, pp. 4892–4905, 2016, doi: 10.1109/TPEL.2015.2480539.

[23] T. Kitaba, "Modeling the system for hybrid renewable energy using highly efficient converters and generator," *CES Transactions on Electrical Machines and Systems*, vol. 8, no. 3, pp. 1–11, Sep. 2024, doi: 10.30941/cestems.2024.00032.

[24] F. A. B. Batista and I. Barbi, "Space vector modulation applied to three-phase three-switch two-level unidirectional PWM rectifier," *IEEE Transactions on Power Electronics*, vol. 22, no. 6, pp. 2245–2252, Nov. 2007, doi: 10.1109/TPEL.2007.909184.

[25] Y. Zhang, J. Fang, F. Gao, T. Song, S. Gao, and D. J. Rogers, "Second-harmonic ripple voltage suppression of integrated single-phase pulsewidth modulation rectifier charging system for EVs," *IEEE Transactions on Power Electronics*, vol. 35, no. 4, pp. 3616–3626, Apr. 2020, doi: 10.1109/TPEL.2019.2937745.

BIOGRAPHIES OF AUTHORS

Shwetha G received B.Tech. in Electrical Engineering from University BDT college of Engineering, Davangere, Karnataka, India in 2014. And Persued M.Tech. Degree from GCE college of Engineering, Ramnagaram in 2016. Now a Ph.D. Research scholar in Electrical Engineering, University Visvesvaraya College of Engineering, K.R.Circle Bangaluru, Karnataka, India 2024. Her current research interests include Design of PWM Rectifier, resonant converters and Electric Vehicle. She can be contacted at email: m.g.shwetha99@gmail.com.

Guruswamy K P is an Associate professor, Dept. of EEE, University Visvesvaraya College of Engineering, Bangaluru, Karnataka, India. He obtained his Bachelor of engineering and ME in Electrical and Electronics Engineering from UVCE College of Engineering, Bangaluru. He was awarded Ph.D. in Electrical Engineering from IIT Roorkee, India. His research interests include Bi-directional DC-DC Power Converters, Digital Control of Multilevel Converters and Resonant Converters. He can be contacted at email: kpg_eeuvce@bub.ernet.in.